

Topics in microphysics of relativistic plasmas

Maxim Lyutikov

Department of Physics, Purdue University, 525 Northwestern Avenue, West Lafayette, IN 47907-2036 USA

INAF - Osservatorio Astrofisico di Arcetri Largo Enrico Fermi 5, I - 50125 Firenze. Italia

The Canadian Institute for Theoretical Astrophysics, University of Toronto, 60 St. George Street Toronto, Ontario, M5S 3H8 Canada

A. Lazarian

Department of Astronomy, University of Wisconsin-Madison, 475 Charter St., Madison, WI 53706

ABSTRACT

Astrophysical plasmas can have parameters vastly different from the more studied laboratory and space plasmas. In particular, the magnetic fields can be the dominant component of the plasma, with energy-density exceeding the particle rest-mass energy density. Magnetic fields then determine the plasma dynamical evolution, energy dissipation and acceleration of non-thermal particles. Recent data coming from astrophysical high energy missions, like magnetar bursts and Crab nebula flares, point to the importance of magnetic reconnection in these objects.

In this review we outline a broad spectrum of problems related to the astrophysical relevant processes in magnetically dominated relativistic plasmas. We discuss the problems of large scale dynamics of relativistic plasmas, relativistic reconnection and particle acceleration at reconnecting layers, turbulent cascade in force-free plasmas. A number of astrophysical applications are also discussed.

1. Introduction

In many astrophysical settings the magnetic field controls the overall dynamics of plasma while the dissipation of magnetic energy may power the high energy emission. The relevant astrophysical settings include magnetars (strongly magnetized neutron stars possessing super-strong magnetic fields), pulsars and pulsar wind nebulae, jets of Active Galactic Nuclei and Gamma-Ray Bursters. All these objects are efficient emitters of X-rays and γ -rays and in the past two decades they have been subjects of intensive observational studies using a number of very successful high energy satellites. These objects seem to share one important property – their plasma is magnetically dominated, that is, the energy density of this plasma is dominated not by the rest mass-energy of matter but by the mass-energy of magnetic field. This is dramatically different from the laboratory plasmas, the magnetospheres of planets, and the interplanetary plasma.

Recently, these topics came to the front of astrophysical and plasma physical research, driven by a series of highly successful high energy mission like, *Swift*, *Fermi*, AGILE satellites and coming on-line of the very high energy γ -ray telescopes like HESS and VERITAS. *A number of observations point to the importance of magnetic dissipation in astrophysical high energy sources*, as we describe below. This signifies a shift of paradigm (from the fluid-dominated point of view) and requires a targeted study of plasma microphysics in a new regime. In this review we outline the related basic plasma physical problems and possible astrophysical applications.

1.1. Crab nebula flares: a new type of astrophysical events

The constancy of the high energy Crab nebula emission has been surprisingly shown to be false by multiple day- to week-long flares, presenting a challenge to standard pulsar wind models (Kennel & Coroniti 1984). During these events, the Crab Nebula gamma-ray flux above 100 MeV exceeded its average value by a factor of several or higher (Abdo et al. 2011; Tavani et al. 2011; Buehler et al. 2012), while in other energy bands nothing unusual was observed (e.g. Abdo et al. 2011; Tavani et al. 2011, and references therein). Additionally, sub-flare variability timescales of ~ 10 hours has been observed (Buehler et al. 2012). The prevailing conclusion from the observations of flares is that flares are associated with the nebular (and not the neutron star) and are mostly likely due to the highest energy synchrotron emitting electrons. Thus, the flares reflect the instantaneous injection/emission properties of the nebular and are not expected to produce a noticeable change in the inverse Compton (IC) component above ~ 1 GeV. One of the most surprising property of the flares is their short time-scale variability, with typical duration two orders of magnitude smaller than the dynamical time-scale of the nebular.

These events question the dominant paradigm of shock acceleration in pulsar wind nebular (Lyutikov 2010; Clausen-Brown & Lyutikov 2012). The key argument in favor of the reconnection origin of the flare is its SED: the peak frequency is above the classical synchrotron limit (de Jager et al. 1996; Lyutikov 2010). This limit comes from assuming the electric field accelerating the emitting particles, E , is less than the emission region magnetic field, or $E = \eta B$, where $0 < \eta < 1$.

$$\mathcal{E}_{\text{ph}}^{\text{max}} = \frac{27}{16\pi} \eta \frac{mhc^3}{e^2} = 236 \eta \text{ MeV}, \quad (1)$$

Instead, these events offer tantalizing evidence in favor of relativistic reconnection (Uzdensky et al. 2011). Clausen-Brown & Lyutikov (2012) suggested that the flare arises due to intermitted reconnection in the downstream region, which produces relativistically moving blobs of plasma. We associate the duration of the flare with stochastically changing properties of plasma within the nebula. Second, the flares are apparently isolated, intermittent high flux events. Such intermittent behavior is often associated with power-law distributions of various kinds generated by astrophysical systems such as magnetically-driven Solar flares (Aschwanden 2005, and references therein).

Relativistic reconnection is a natural flaring mechanism in PWNe. The flare can be due to a highly localized emission region, or blob, so that the flare observables determine the intrinsic properties of the emission region. The natural flaring mechanism in this category is relativistic magnetic reconnection, which has been invoked by Crab Nebula flare models (Uzdensky et al. 2011) and fast flaring models in gamma-ray bursts (GRBs) and active galactic nuclei (AGN, Lyutikov 2006b; Giannios et al. 2009b).

In reconnection, the magnetic energy of a localized region, a current sheet, is converted to random particle energy, (possibly) bulk relativistic motion, and radiation (for studies on reconnection in highly magnetized relativistic plasmas, see Lyutikov & Uzdensky 2003; Lyubarsky 2005; Uzdensky et al. 2011; McKinney & Uzdensky 2012). Reconnection in PWNe has already been studied in the past as a possible resolution of the well known σ -problem (Lyubarsky 2003; Komissarov 2012). In a similar vein, Lyutikov (2010) proposes a model in which, reconnection occurs primarily along the rotation axis and equatorial region well beyond the light cylinder, thus qualitatively reproducing the jet/equatorial wisp morphology of the nebula.

We have developed (Clausen-Brown & Lyutikov 2012) a statistical model of the emission from Doppler boosted reconnection mini-jets, looking for analytical expressions for the moments of the resulting nebula light curve (e.g. time average, variance, skewness). The light curve has a flat power spectrum that transitions

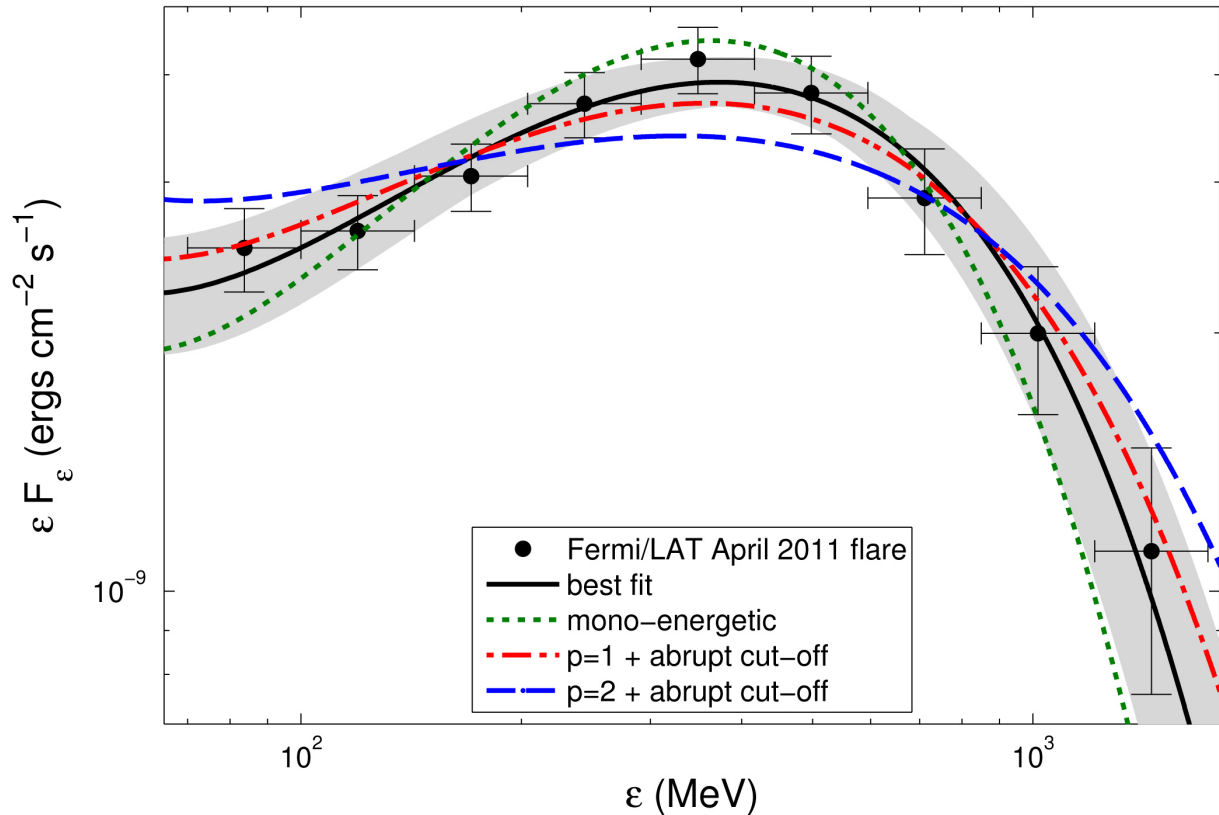


Fig. 1.— The Fermi/LAT data from the most energetic part of the April 2011 Crab flare (Buehler et al. 2012) with the corresponding best fit curve and SEDs from three different electron energy distributions: a $p = 1$ power-law with an abrupt cut-off, the same for $p = 2$, and a mono-energetic electron distribution (Clausen-Brown & Lyutikov 2012). The shaded area represents the one- σ error region. The data favor steep injection spectrum with a pile-up, consistent with acceleration in reconnection regions.

at short timescales to a decreasing power-law of index 2, Fig. 2. The flux distribution from mini-jets follows a decreasing power-law of index ~ 1 , implying the average flux from flares is dominated by bright rare events. The predictions for the flares’ statistics can be tested against forthcoming observations. We find the observed flare spectral energy distributions (SEDs) have several notable features: A hard power-law index of $p \lesssim 1$ for accelerated particles that is expected in various reconnection models, including some evidence of a pile-up near the radiation reaction limit. Also, the photon energy at which the SED peaks is higher than that implied by the synchrotron radiation reaction limit, indicating the flare emission regions’ Doppler factors are \gtrsim few. Magnetic reconnection can be an important, if not dominant, mechanism of particle acceleration within the nebula.

If magnetic reconnection is what causes the flares, the reconnection process itself may leave a particular imprint on the SED in the form of a hard electron distribution. If much of the synchrotron emission occurs from particles near the synchrotron limit, then the emitting particles will display a SED that is close the single-particle synchrotron SED, see Fig. 1. The best flare SED observations to date are 11 SEDs taken during the April 2011 by Fermi/LAT team (Buehler et al. 2012). They were fitted with an empirical function

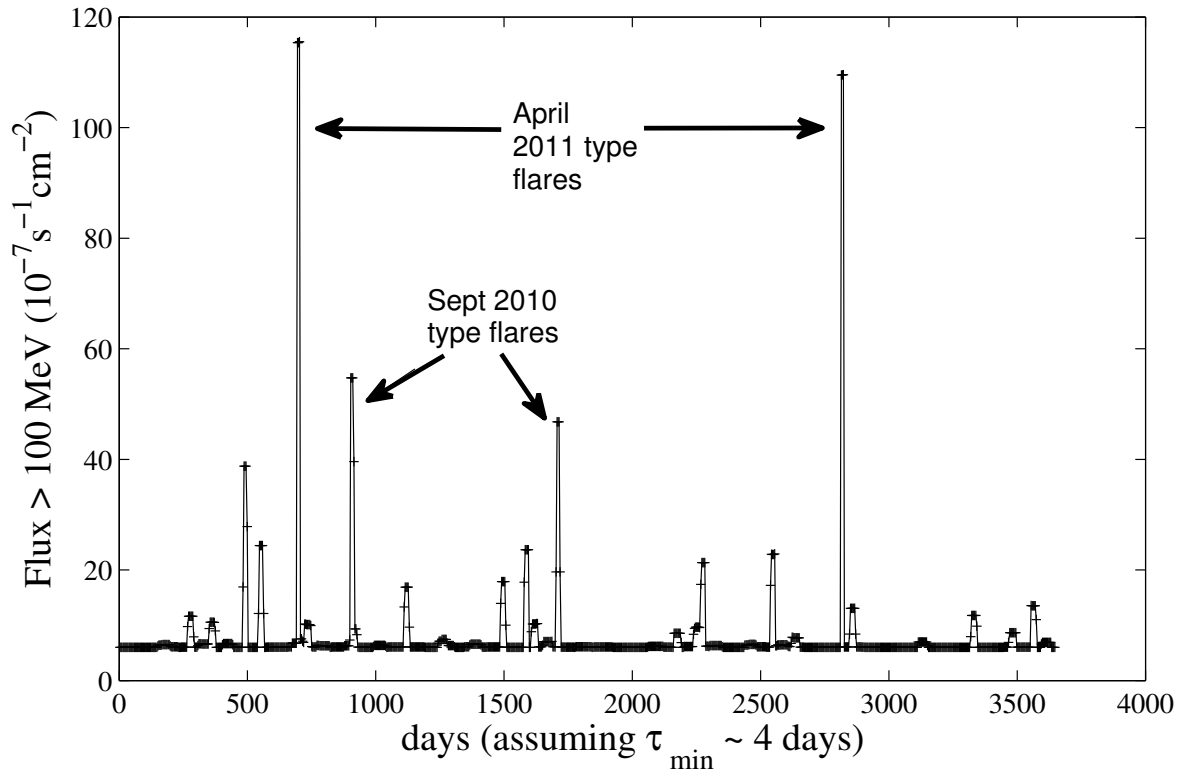


Fig. 2.— Ten year simulated Crab nebula light curve with the reconnection model of Crab flares. The “April 2011 type flares” represent flares with increases of ~ 30 over the nebular average as found in Buehler et al. (2012).

of the form $\epsilon F_\epsilon \propto \epsilon^a \exp(\epsilon/\epsilon_c)$, where ϵ represents photon energy, and different values for the normalization and ϵ_c were used for each SED. The parameter a was assumed to be constant for all of the SEDs, and its best fit value is $a = 0.73 \pm 0.12$. The SED taken during the most luminous part of the flare, with a ϵF_ϵ maximum of $\sim 4 \times 10^{-9} \text{ ergs}^{-1} \text{ s}^{-1}$ at a peak photon energy of $\epsilon_{\text{peak}} = 375 \pm 26 \text{ MeV}$, probably constrained the best fit value of a the most.

1.2. Magnetar Giant Flares.

In phenomena possibly related to Crab flares, two closely related classes of young neutron stars – Anomalous X-ray Pulsars (AXPs) and the Soft Gamma-ray Repeaters (SGRs) – both show X-ray flares and, once localized, quiescent X-ray emission (Kouveliotou et al. 1998, Gavriil *et al.* 2002; for recent review see Woods & Thompson (2004)). Their high energy emission is powered by the dissipation of their super-strong magnetic fields, $B > 10^{15} \text{ G}$ (Thompson & Duncan 1996). Two models of GFs are proposed. First, a GF may result from a *sudden untwisting of the internal magnetic field* (and twisting-up of the external magnetic field, Thompson & Duncan 1995, 2001). Alternatively, a *slow* untwisting of the internal magnetic field may lead to a gradual twisting of magnetospheric field lines, on time scales much longer than the GF, until it reaches

a dynamical stability threshold due to increasing energy associated with the current-carrying magnetic field. Then follows a *sudden relaxation* of the twist outside the star and an associated dissipation and a change of magnetic topology lead to a GF, in analogy with solar flares and Coronal Mass Ejections (CMEs) (Lyutikov 2006a).

The observed sharp rise of γ -ray flux during GF, on a time scale similar to the Alfvén crossing time of the inner magnetosphere, which takes ~ 0.25 msec (Palmer *et al.* 2005). This unambiguously points to the magnetospheric origin of GFs, presumably during reconnection event in the magnetically-dominated magnetosphere (Lyutikov 2006a).

The processes that cause magnetar X-ray flares (and possibly the persistent emission) may be similar to those operating in the solar corona. The energy of magnetar flares is accumulated inside the neutron star at the moment of its formation in the form of interior electric currents. These currents are then slowly pushed into the magnetosphere, gated by slow, plastic deformations of the neutron star crust. This leads to gradual twisting of the magnetospheric field lines, on time scales much longer than the magnetar’s GF, and creates active magnetospheric regions similar to the Sun’s spots. Initially, when the electric current (and possibly the magnetic flux) is pushed from the interior of the star into the magnetosphere, the latter slowly adjusts to the changing boundary conditions. As more and more current is pushed into the magnetosphere, it eventually reaches a point of dynamical instability. The loss of stability leads to a rapid restructuring of magnetic configuration, on the Alfvén crossing time scale, to the formation of narrow current sheets, and to the onset of magnetic dissipation. As a result, a large amount of magnetic energy is converted into the kinetic and bulk motion and radiation.

Observationally, a number of data point to the reconnection origin of the magnetar flares. Other predictions of the model, confirmed by observations are (i) the post-flare magnetosphere has a simpler structure, as the pre-flare network of currents has been largely dissipated; (ii) its spectrum is softer, since the hardness of the spectrum is a measure of the current strength in the bulk of magnetosphere (Thompson *et al.* 2002; Lyutikov & Gavriil 2005), with softer spectra corresponding to a smaller external current; and (iii) the spin-down rate, which depends on the amount of electric current flowing through the open field lines, decreases. The observations of two recent GFs, in SGR 1900+14 and SGR 1806-20, fully agree with these predictions. In both cases the persistent flux increased by a factor of two, its spectrum hardened (the power law index decreased from 2.2 to 1.5), and the spin-down rate increased in the months leading to the flare (Mereghetti *et al.* 2005). In the post-flare period, the pulsed fraction and the spin-down rate have significantly decreased and the spectrum softened (Rea *et al.* 2005). All these effects imply an increase of the external current before, and a decrease after the flare (Lyutikov 2006a).

1.3. Reconnection in magnetized jets of Active Galactic Nuclei and Gamma Ray Bursts

Recent observations of AGNs in GeV and TeV energy range have raised new questions regarding the parameters of the central engine, and the location and kinematics of the high energy γ -ray, as well as X-ray and radio emission zones. In particular, the rapid flares reported for Mrk 501 and PKS 2155-304, on timescales of 3-5 minutes (Albert 2007; Aharonian 2007) imply an emitting size smaller than the gravitational radius $t_{lc} \sim$ hours of the supermassive black holes of these blazars. This indicates a very high Doppler factors δ , exceeding $\delta = 100$. A similar estimate also comes from the requirement that the TeV photons escape the production region.

While highly relativistic motion may appear to be a cure-all, the bulk Lorentz factor Γ can be directly

constrained by VLBI observations of bright blobs moving with apparent speeds on the sky, β_{app} , that appear to be superluminal. This type of motion occurs when the emitting region is moving relativistically and close to the line of sight (Rees 1966). The apparent motion can exceed c due to propagation effects. If a blob is moving along with the bulk flow of a jet and its velocity vector makes an angle, θ_{ob} , with the line of sight, then its apparent motion transverse to the line of sight will be: $\beta_{app} = \frac{\beta_{\Gamma} \sin \theta_{ob}}{1 - \beta_{\Gamma} \cos \theta_{ob}}$. The maximum β_{app} can reach is $\beta_{\Gamma} \Gamma$ when $\theta_{ob} \cong 1/\Gamma$. Thus, if the blob motion corresponds to the underlying bulk motion of the jet, measuring β_{app} can constrain the possible bulk Lorentz factor, Γ .

Following the suggestion by Lyutikov (2006b), a number of authors (Giannios et al. 2009b; Ghisellini & Tavecchio 2008; Lazar et al. 2009; Kumar & Narayan 2009) proposed that fast time scale variability both in AGNs and GRBs is produced by "mini-jets", compact emitting regions that move relativistically *within* a jet of bulk $\Gamma \sim 10$ (in case of AGNs; for GRBs $\Gamma \sim 100$). Thus, the emission is beamed in the bulk outflow frame, *e.g.* due to relativistic motion of (using pulsar physics parlance) "fundamental emitters".

In GRBs, claims of high polarization (Coburn & Boggs 2003; Willis *et al.* 2005) offer direct measurements of the possibly dominant large-scale magnetic field. If confirmed, these observations argue in favor of magnetic reconnection as the main particle acceleration mechanism.

1.4. Reconnection in the Double Pulsar system PSR J0737–3039

Detection by McLaughlin *et al.* (2004a) of drifting sub-pulses of pulsar B in the Double Pulsar system PSR J0737–3039 with the frequency related to A period, presents an excellent opportunity to use Pulsar B as a probe of Pulsar A wind properties at ~ 1000 light cylinder radii of A, many orders of magnitude closer that have been possible so far. In particular, the fact that the observed modulation is at the frequency of A, and not a double frequency, already can be used as an indication that a large fraction of A wind is carried by relativistic MHD waves so that *directions* of electric and/or magnetic fields are important, not only total pressure of the wind.

A possible explanation is that the modulation of B by A is due to reconnection between magnetic fields in the wind and in the B magnetosphere. When magnetospheric field lines connect to the wind's magnetic field, they are "dragged" by the wind. Half a spin period of pulsar A later, when the wind's magnetic field changes polarity, the magnetospheric magnetic field disconnects from the wind and relaxes back to the position given by the impenetrable conductive boundary conditions. As the radio emission is produced along the local direction of a magnetic field, this periodic "dragging" and relaxation.

2. Dynamic force-free plasma

In astrophysical settings the local microscopic plasma time scale (*e.g.* plasma frequency) is much shorter than the global dynamical time scales and there is plenty of charges available to screen the component of electric field along the magnetic field. In addition, astrophysical plasma is usually collisionless, making it an extremely good conductor. In addition, there is plenty of charges available to screen the component of electric field along the magnetic field $\mathbf{E} \cdot \mathbf{B} = 0$. Even in the extreme cases, when plasma may not be able to short out parallel electric field due to lack of available charges (charge separated flows) various radiative process (*e.g.* emission of curvature photon or through inverse Compton scattering) may lead to what is known as vacuum breakdown: abundant production of electron-positron pairs. The newly born pairs will

create a charge density that would shut-off the accelerating electric field. The typical potential difference $\Delta V_{\text{vac}} \sim kT/e$ needed to break down the vacuum in a GRB is typically in the MV-GV range. This is often orders of magnitude smaller than typically available EMF ($\sim 10^{15} - 10^{16}$ eV for pulsars, $\sim 10^{18} - 10^{20}$ eV for AGNs and GRBs).

The properties of plasma in the magnetospheres of pulsars and magnetars, pulsar winds, AGN and GRB jets are very different from those of more conventional Solar and laboratory plasmas. The principal difference is that it is relativistically strongly magnetized. In order to describe the level of magnetization it is convenient to use the so-called magnetization parameter $\sigma = 2(u_B/u_p)$, where $u_B = B^2/8\pi$ is the magnetic energy density and $u_p = \rho c^2$ is the rest mass-energy density. In traditional plasmas this parameter is very small. On the contrary, in some astrophysical settings it is likely to be very large. For example, in magnetars

$$\frac{\omega_B R_{NS}}{c} \left(\frac{m_e}{m_p} \right) \sim 10^{13} \leq \sigma \leq \frac{\omega_B}{\Omega} \left(\frac{m_e}{m_p} \right) \sim 10^{16} \quad (2)$$

(the upper limit corresponds to the Goldreich-Julian density of electron-ion plasma whereas the lower limit corresponds to the poloidal current producing the toroidal magnetic field of the same order as the poloidal one. Here $\omega_B = eB/m_e c$ is the cyclotron frequency, B is the magnetic field at the neutron star surface, R_{NS} is the neutron star radius, and Ω is its rotational frequency.

The parameter regime of highly magnetized plasma, $\sigma \gg 1$, implies that (i) the inertia of this plasma is dominated by the magnetic field and not by the particle rest mass, $B^2/8\pi \gg \rho c^2$, (ii) the propagation speed of Alfvén waves approaches the speed of light, (iii) the conduction current flows mostly along the magnetic fieldlines, (iv) the displacement current $(c/4\pi)\partial_t \mathbf{E}$ may be of the same order as the conduction current, \mathbf{j} , (v) the electric charge density, ρ_e , may be of the order of j/c . These are very different from the properties of laboratory plasmas, plasmas of planetary magnetospheres, and the interplanetary plasma, the cases where plenty of experimental data and theoretical results exist.

The large expected value of σ (or small $1/\sigma$) may be used as an expansion parameter in the equations of relativistic magnetohydrodynamics. The zero order equations describe the so-called relativistic force-free approximation. One may see this limit as the model where massless charged particles support currents and charge densities such that the total Lorentz force vanishes all the time (this also insures the ideal condition $\mathbf{E} \cdot \mathbf{B} = 0$.) This allows one to related the current to electro-magnetic fields (Gruzinov 1999)

$$\mathbf{J} = \frac{c}{4\pi} \frac{(\mathbf{E} \times \mathbf{B})\nabla \cdot \mathbf{E} + (\mathbf{B} \cdot \nabla \times \mathbf{B} - \mathbf{E} \cdot \nabla \times \mathbf{E})\mathbf{B}}{B^2} \quad (3)$$

This may be considered as the Ohm's law for relativistic force-free electro-dynamics. (Note that this implies that the invariant $\mathbf{E} \cdot \mathbf{B} = 0$ and that electromagnetic energy is conserved, $\mathbf{E} \cdot \mathbf{J} = 0$.)

Under stationary and axisymmetric conditions, these equations guarantee that the angular velocity Ω is conserved along field lines. They also require a space charge density $\rho = \nabla \cdot \mathbf{E}/(4\pi)$ of magnitude $\sim \Omega B/c$ to develop. (Formally this, like the equation $\nabla \cdot \mathbf{B} = 0$, is just an initial condition.)

In the non-relativistic plasma the notion of force-free fields is often related to the stationary configuration attained asymptotically by the system (subject to some boundary conditions and some constraints, *e.g.* conservation of helicity). This equilibrium is attained on time scales of the order of the Alfvén crossing times. In strongly magnetized relativistic plasma the Alfvén speed may become of the order of the speed of light c , so that crossing times becomes of the order of the light travel time. But if plasma is moving relativistically its state is changing on the same time scale. This leads to a notion of dynamical force-free fields.

The force-free condition can be re-expressed by setting the divergence of the electromagnetic stress tensor to zero. This form has the merit that it brings out the analogy with fluid mechanics. Electromagnetic stress pushes and pulls electromagnetic energy which moves with an electromagnetic velocity $\mathbf{E} \times \mathbf{B}/B^2$, perpendicular to the electric and magnetic fields. This is the velocity of the frames (only defined up to an arbitrary Lorenz boost along the magnetic field direction) in which the electric field vanishes, (provided that the first electromagnetic invariant $B^2 - E^2 > 0$).

The limit $\sigma \rightarrow \infty$ is somewhat reminiscent of subsonic hydrodynamics as both the fast speed and the Alfvén speed approach the speed of light. For example, in case of slow processes, taking place on time scales much longer than light travel time, the Maxwell’s equations may be written as continuity and momentum conservation (Komissarov et al. 2007)):

$$\partial_t \rho + \nabla \cdot (2\rho \mathbf{V}) = 0, \quad \partial_t \rho \mathbf{V} + \nabla \cdot \left(-\frac{\mathbf{B} \otimes \mathbf{B}}{4\pi} + \mathbf{I} \frac{B^2}{8\pi} \right) = 0. \quad (4)$$

where $\rho = B^2/8\pi c^2$ is the effective mass density of the electromagnetic field and $\mathbf{V} = \mathbf{E} \times \mathbf{B}/B^2$ is the drift speed of charged particles, This closed system of equations is very similar to non-relativistic MHD. This observation provides an interesting insight into the dynamics of two very different dynamical systems.

2.1. Time-dependent hyperbolic Grad-Shafranov equations

Lyutikov (2011) demonstrated that the time evolution of the axisymmetric force-free magnetic fields can be expressed in terms of the hyperbolic Grad-Shafranov equation, under the assumption that the fields remain axially-symmetric. Qualitatively, there two separate types of non-stationarity: (i) due to the variations of the current $I(t)$ for a given shape of the flux function; (ii) due to the variations of the shape of the flux function for a given current I . Using these equations it is possible to find exact non-linear time-dependent Michel-type (split-monopole) structure of magnetospheres, *e.g.*, driven by spinning and collapsing neutron star in Schwarzschild geometry:

$$\begin{aligned} B_r &= \left(\frac{R_s}{r} \right)^2 B_s, \quad B_\phi = -\frac{R_s^2 \Omega \sin \theta}{r} B_s, \quad E_\theta = B_\phi \\ j_r &= -2 \left(\frac{R_s}{r} \right)^2 \cos \theta \Omega B_s \\ P &= (1 - \cos \theta) B_s R_s^2 \\ \Phi &= -P\Omega \\ I &= -\frac{P(P - 2B_s R_s^2)\Omega}{2B_s R_s^2} = \frac{1}{2} B_s R_s^2 \Omega \sin^2 \theta \end{aligned} \quad (5)$$

where P is the flux function, and Φ is the electric potential and $\Omega = \Omega(r - t)$ is *an arbitrary function*. Thus, we found exact solutions for time-dependent non-linear relativistic force-free configurations. Though the configuration is non-stationary (there is a time-dependent propagating wave), the form of the flux surfaces remains constant.

2.2. Limitations of force-free approach

The generic limitation of the force-free formulation of MHD is that the evolution of the electromagnetic field leads, under certain conditions, to the formation of regions with $E > B$ (*e.g.* Uzdensky 2003), since

there is no mathematical limitation on $B^2 - E^2$ changing a sign under a strict force-free conditions. In practice, the particles in these regions are subject to rapid acceleration through $\vec{E} \times \vec{B}$ drift, following by a formation of pair plasma via various radiative effects and reduction of the electric field. Thus, regions with $E > B$ are necessarily resistive. This breaks the ideal assumption and leads to the slippage of magnetic field lines with respect to plasma. In addition, evolution of the magnetized plasma often leads to formation of resistive current sheets, with the similar effect on magnetic field.

As a simple example demonstrating that the dynamical system described by the relativistic force-free limit has a natural tendency to violate the physical requirement of a negative first electromagnetic invariant, $E^2 - B^2 < 0$, consider a resistive decay of a line current. Suppose at time $t = 0-$ there is a line current I_0 that decays for times $t > 0$ according to $I = I_0(1 - t/\tau)$. This launches an outgoing rarefaction wave in which the EM field are given by

$$\begin{aligned} B_\phi &= \frac{I_0}{2\pi r} \left(1 - \frac{\sqrt{t^2 - r^2}}{\tau} \right) \\ E_z &= -\frac{I_0}{2\pi\tau} \ln \frac{t - \sqrt{t^2 - r^2}}{r} \end{aligned} \quad (6)$$

(for $r < t$). The resulting radial inward velocity, $v_r = E_z/B_\phi$ at some moment becomes larger than the speed of light. This example illustrates an important point: in force-free approximation plasma tends to develop dissipative regions where $E \rightarrow B$. This regions can develop non-locally, far from the cause that initiated the plasma motion (resistive decay at $r = 0$).

Another generic limitation of the force-free approach is related to the structure of the current sheet. Since in the force-free limit the plasma pressures are neglected, nothing prevents formation of very thin and thus highly dissipative current sheets. As a result, numerical models then can produce exceptionally high dissipation rates (*e.g.* Gruzinov 2012; Lehner et al. 2011). If small kinetic pressure is taken into account (*e.g.* Lyutikov & McKinney 2011; Tchekhovskoy & Spitkovsky 2012), the reconnection rate drops considerably. Another approach that allows (partial) stabilization of the current sheet is the resistive force-free plasma dynamics, which we discuss next.

3. Dissipation in highly magnetized plasmas

3.1. Tearing mode in force-free plasma

One of the most important resistive instabilities in a conventional plasma is the so-called tearing instability. This is one of the principle unstable resistive modes, which plays a key role in various TOKAMAK discharges like the sawtooth oscillations and the major disruptions (*e.g.* Kadomtsev 1975), and leads to the unsteady reconnection of Solar flares (*e.g.* Shivamoggi 1985; Aschwanden 2002) and Earth's magnetotail (*e.g.* Galeev *et al.* 1978). The most important property of the tearing instability is the growth time that is much shorter than the resistive time.

In addition to being magnetically-dominated, microscopic plasma processes, like particle collisions or plasma turbulence, may contribute to resistivity and thus make plasma non-ideal. Resistivity will result in the decay of currents supporting the magnetic field; this, in turn, will influence the plasma dynamics. Introduction of resistivity into force-free formulation is not entirely self-consistent. The reason is that in force-free plasma the velocity along the field is not defined. Since plasma resistivity must be defined in the plasma rest-frame this creates a principal ambiguity.

The force-free tearing mode has been considered by Lyutikov (2003) (see also Gruzinov 2007; Li et al. 2012, for a somewhat different formulation of resistive force-free plasma). Lyutikov (2003) found that similar to the non-relativistic case, the resistive force-free current layers are unstable toward the formation of small-scale dissipative current sheets. He has also found that the growth rate of tearing instability, $\tau = \sqrt{\tau_d \tau_a}$, is intermediate between the short Alfvén time scale τ_a (which equals to the light crossing time in the force-free regime) and the long resistive time scale $\tau_d = l^2/\eta$, where l is the width of the current layer. This is exactly the same expression as in the non-relativistic case, which is rather surprising given the fact that the dynamic equations of force-free plasma are very different from the equations of non-relativistic MHD.

Numerical modeling of the tearing instability in strongly magnetized plasma Komissarov et al. (2007) (see Fig. 3.) fully confirm the analytical estimates.

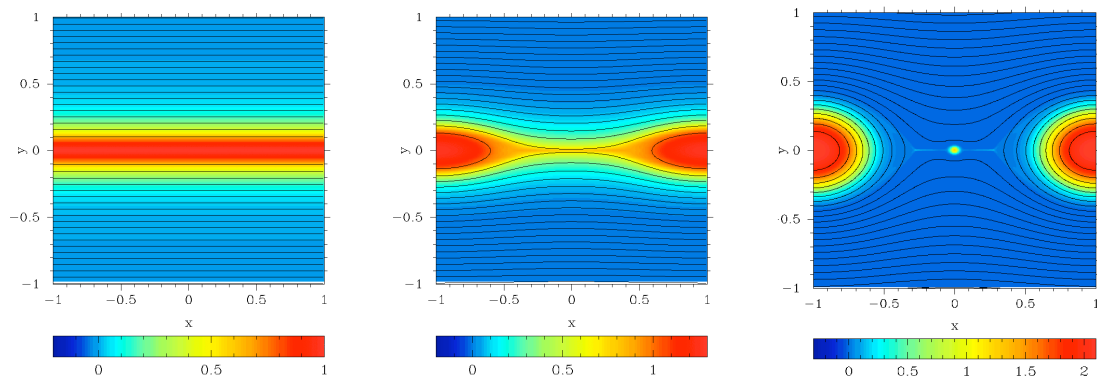


Fig. 3.— Numerical simulations of the tearing instability in force-free plasma. The color images show the distribution of B_z and the contours show the magnetic field lines. In this simulations the perturbation has the wavelength corresponding to the maximum growth rate, $\tau \simeq \sqrt{\tau_d \tau_c}$, where τ_d is the resistive time and τ_c is the light crossing time of the current layer. The Lundquist number $L_u = \tau_d/\tau_c = 10^3$.

In high Reynolds number plasma it is expected that tearing developing into turbulence. This has been observed in both PIC and MHD recent simulations (see below).

3.2. X-point collapse in force-free plasma

Consider a vicinity of an X-point. The non-current-carrying configuration has null lines intersecting at 90 degrees. Following the work on the collapse of a non-relativistic X-point (Dungey 1953; Imshennik & Syrovatskivi 1967; Priest & Forbes 2000), let us assume that the initial configuration is squeezed by a factor λ , so that the initial configuration has a vector potential $A_z \propto x^2 - y^2/\lambda^2$. In addition, we assume that there is an axial constant magnetic field B_z .

We are looking for time evolution of a vector potential of the type

$$A_z = - \left(\frac{x^2}{a(t)^2} - \frac{y^2}{b(t)^2} \right) \frac{B_0}{2L}, \quad (7)$$

where parameters B_0 and L characterize the overall scaling of the magnetic field and the spacial scale of

the problem.

The initial condition for the squeezed X-point and the ideal condition then require

$$\begin{aligned} b(t) &= \lambda/a(t) \\ \Phi &= xy \frac{B_z}{c} \partial_t \ln a \end{aligned} \quad (8)$$

(Since $\Delta\Phi = 0$ there is no induced charge density.) Parameter a characterizes the “squeezeness” of the configuration; $a = 1$ is the current-free case.

Faraday’s law is then an identity, while the induction equation in the limit $x, y \rightarrow 0$ gives

$$\partial_t^2 \ln a = \mathcal{A} \left(\frac{a^4 - \lambda^2}{\lambda^4} \right), \quad \mathcal{A} = \frac{c^2 B_0^2}{L^2 B_z^2} \quad (9)$$

Solutions of the equations (9) show that $a(t)$ has a finite time singularity for $\lambda < 1$: in finite time a becomes infinite. At the moment when one of the parameters a or b becomes zero, the current sheet forms, see Fig. 4.

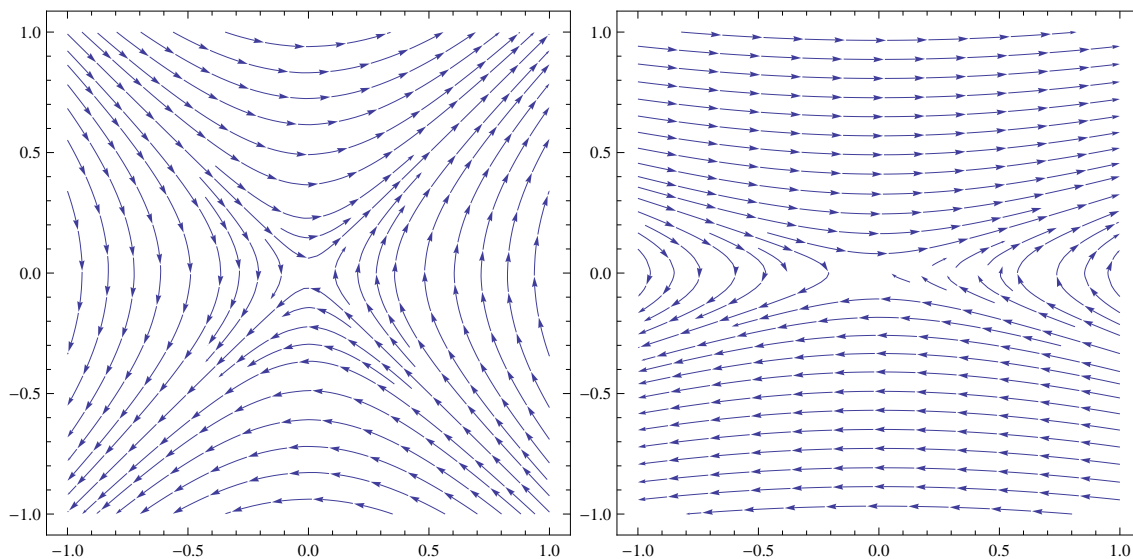


Fig. 4.— Structure of the magnetic field in the $x - y$ plane during X-point collapse in force-free plasma. The initial configuration on the left is slightly “squeezed”. On dynamical time scale the X-point collapses to form a current sheet, right figure. The structure of the electric field in the $x - y$ plane does not change during the collapse and qualitatively resembles the $t = 0$ configuration of the magnetic field.

For small times $t \rightarrow 0$ (when $|a - 1| \ll 1$), with initial conditions $a(0) = 1$, $a'(0) = 0$, and assuming that the initial “squeezing” is small, $\lambda = 1 - \epsilon$, $\epsilon \ll 1$, the solution is

$$a = 1 + \epsilon \sinh^2 \left(\frac{ct B_0}{L B_z} \right) \quad (10)$$

Thus, the typical collapse time is

$$\tau \sim \frac{L B_z}{c B_0} \quad (11)$$

is of the order of the Alfvén (light) crossing time of the initial configuration. At these early times the electric field grows exponentially

At early times the particle drift follows a trajectory in the $x-y$ plane $y \propto 1/x$. During the final collapse, in the limit $a \rightarrow \infty$, the particle distribution is further squeezed towards the neutral layer, $y \propto 1/(a^2 \sqrt{\ln x})$ (though in this limit the drift approximation becomes inapplicable.) This shows that the X-point is stretched in one direction and is compressed in the other direction (note that $\nabla \mathbf{v} = 0$ - collapse is incompressible at the initial stage).

Thus, in an ideal relativistic force-free plasma the X-point undergoes a finite time collapse. At the same time, particles are squeezed by the electromagnetic drift towards the neutral layer. The assumption of the force-free plasma will be broken down when the inflow velocity would become of the order of the Alfvén velocity. Then, the maximum electric field is $E \sim \beta_A B_0$ which is of the order of B_0 , magnetic field in the bulk, for $\sigma \geq 1$. The collapse occurs faster for small axial field $B_z \leq B_0$.

3.3. Stationary relativistic reconnection

Magnetic reconnection is widely recognized as a very important phenomenon in many laboratory and astrophysical plasmas (Biskamp 2000, Priest & Forbes 2000). It has been studied very extensively over the last 40 years, and a significant progress has been made. However, historically, the main applications of the reconnection theory were confined to Solar physics, Earth’s magnetosphere and the fusion projects. In all these cases, the magnetic energy density is much smaller than the particle rest mass-energy density, and the characteristic speeds are much less than the speed of light. Therefore it is not surprising that most of the progress has been made in the non-relativistic regime.

The analytical studies of dissipative effects in resistive magnetically dominated plasmas, though limited in their generality, provide an important first step towards the full understanding of the plasma dynamics under these extreme conditions and will serve as a guide for numerical investigations.

The first step is the generalization of non-relativistic models to the new regime Lyutikov & Uzdensky (2003); Lyubarsky (2005) According to Lyutikov & Uzdensky (2003), the relativistic theory of the simplest model of magnetic reconnection — the Sweet–Parker model — involves two very large parameters: the Lundquist number, L_u , and the magnetization parameter σ . The simplest Sweet–Parker model of relativistic reconnection cannot be built self-consistently. The reason is that the convention non-relativistic model operates only with conservation laws, and not with the dynamical structure. In the relativistic case the conservation of energy then predicts acceleration to high Lorentz factors (Lyutikov & Uzdensky 2003), but this would lead to large pressure drop and would violate a force-balance across the current sheet (Lyubarsky 2005).

Overall properties of stationary relativistic reconnection (like inflow and outflow velocities, Sweet-Parker versus Petschek models) remains an open question (for a recently review see Hoshino & Lyubarsky 2012). The shift in our understanding of non-relativistic reconnection layers, in particular as we discuss in more detail later, the importance of turbulence (Lazarian & Vishniac 1999) that is present in most astrophysical systems due to numerous instabilities that prey on high Reynolds number velocity fluids.

Interestingly enough, reconnection itself creates turbulence, which can be the cause of “reconnection instability” described in Lazarian & Vishniac (1999, 2009), which develops when the initial level of turbulence in the system is low or even the magnetic fields are originally laminar. As the outflow gets turbulent, the

level of turbulence in the system and the reconnection rate increases inducing the positive feedback. This process may result in bursty reconnection of the time seen in solar flares, where the initial state of turbulence is low. This process can be also a driver of other dramatic energy bursts, e.g. gamma ray bursts (Lazarian et al. 2003, Zhang & Yan 2011, Lazarian & Yan 2012).

It is important that the initially laminar reconnection layer is subject to the tearing mode instability¹ Loureiro et al. (2007), which both drive reconnection and ensure the turbulent state of the 3D reconnection layer (see Karimabadi 2013, Lazarian & Karimabadi 2013, Beresnyak 2013). All this puts in doubt many stationary and laminar reconnection models. Indeed, as described above, in astrophysics the relativistic reconnection is invoked for highly non-stationary processes and a laminar state of astrophysical fluid is more of an exception rather than a rule. Thus, one might expect that in the relativistic regime the current sheet is being fragmented and broadened by turbulence or/and subject to tearing.

3.3.1. Reconnection in the presence of turbulence

Properties of fluids are known to be strongly affected by turbulence. For instance, diffusion in turbulent fluids does not depend on molecular diffusivity. Thus, it is important to understand what can be the role of turbulence for the diffusion of magnetic field and reconnection that this transport can entail within relativistic plasmas. Below we provide arguments suggesting that turbulence can make magnetic reconnection fast.

In terms of non-relativistic fluids, the predictive model of turbulent reconnection was presented in Lazarian & Vishniac (1999) [henceforth LV99]. LV99 considered reconnection in the presence of sub-Alfvénic turbulence in magnetized plasmas. They identified stochastic wandering of magnetic field-lines as the most critical property of MHD turbulence which permits fast reconnection. As illustrated in Figure 5, this line-wandering widens the outflow region and alleviates the controlling constraint of mass conservation²

One can argue that the LV99 model that was shown to make reconnection fast carries over to relativistic fluids the same way as other, e.g. Sweet-Parker model does. In fact, it is clear from Figure 5 that LV99 generalizes the Sweet-Parker model for the case of turbulent magnetic fields. The limitation that makes the Sweet-Parker reconnection slow both in relativistic and non-relativistic cases stems from the fact that the thickness of the outflow region is limited by effects related to plasma conductivity. These effects are related to microscopic scales and make $\Delta \ll L$ for the case of laminar fluids. In the case of LV99 reconnection the outflow is determined by macroscopic field wandering and therefore the Δ can get comparable with L . As the mass conservation dictates that the reconnection velocity is

$$V_{rec} \approx V_A \Delta / L \tag{12}$$

LV99 reconnection gets fast and it depends only on the intensity and injection scale of turbulence. In the relativistic limit V_A approaches the velocity of light and therefore one can expect Eq. (12) to hold with

¹The estimates of the tearing mode in highly relativistic plasmas (see §3.1) indicate that the mode growth rate (surprisingly) follows the non-relativistic scaling.

²The LV99 model is radically different from its predecessors which also appealed to the effects of turbulence. For instance, unlike Speiser (1970) and Jacobson & Moses (1984) the model does not appeal to changes of microscopic properties of plasma. The nearest progenitor to LV99 was the work of Matthaeus & Lamkin (1985) Matthaeus & Lamkin (1986), who studied the problem numerically in 2D MHD and who suggested that magnetic reconnection may be fast due to a number of turbulence effects, e.g. multiple X points and turbulent EMF. However, these papers did not address the important role of magnetic field-line wandering, and did not obtain a quantitative prediction for the reconnection rate, as did LV99.

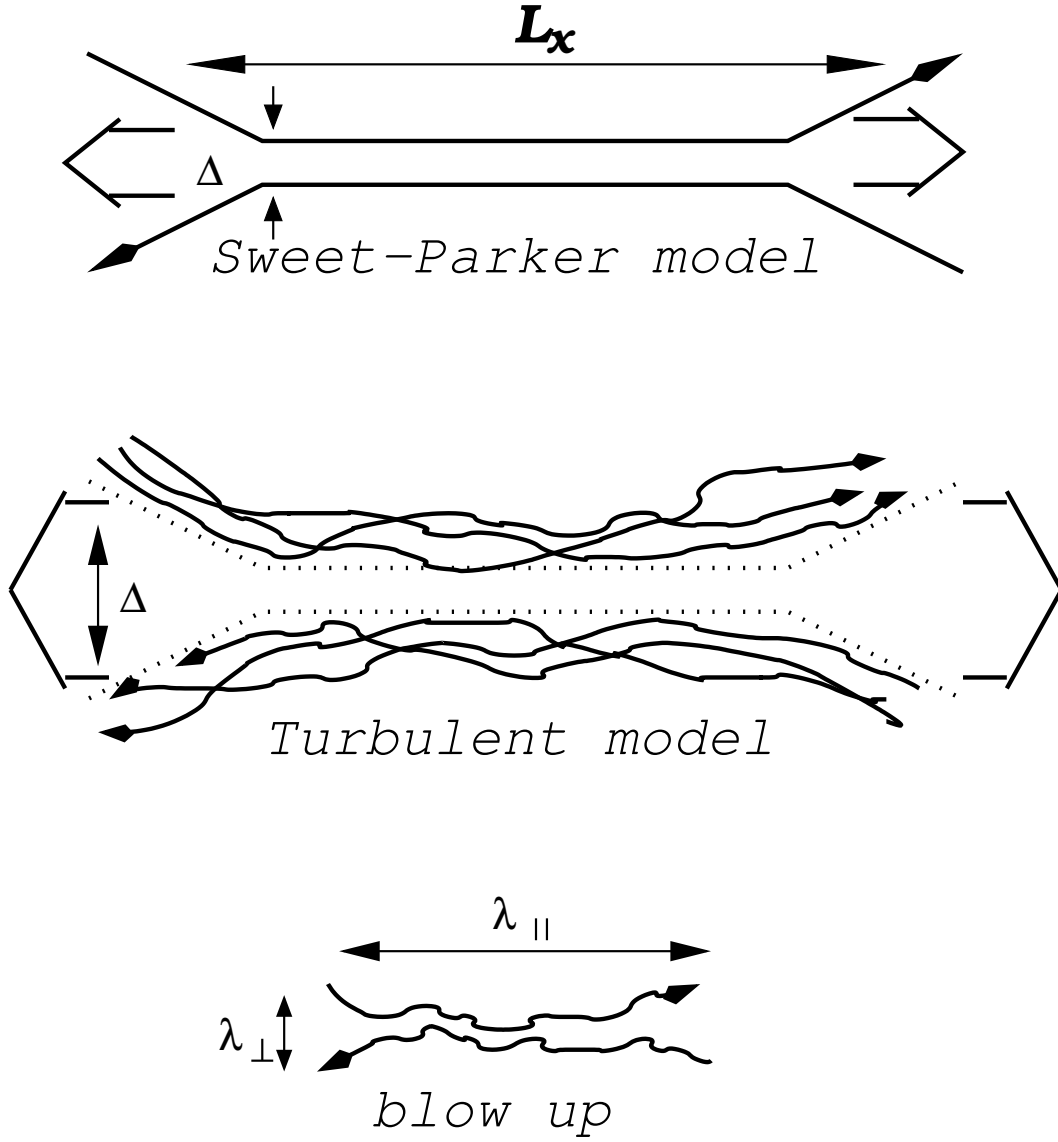


Fig. 5.— Upper plot: Sweet-Parker model of reconnection. The outflow is limited by a thin slot Δ , which is determined by Ohmic diffusivity. The other scale is an astrophysical scale $L_{x,i}$. Middle plot: Reconnection of weakly stochastic magnetic field according to LV99. The Goldreich-Sridhar (1995) model of MHD turbulence is used to account for the stochasticity of magnetic field lines. The outflow in the LV99 theory is limited by the diffusion of magnetic field lines, which depends on field line stochasticity. Lower plot: An individual small-scale reconnection region. The reconnection over small patches of magnetic field determines the local reconnection rate. The global reconnection rate is substantially larger as many independent patches come together. From Lazarian et al. (2004).

the change of V_A to c . At the same time, the exact scaling of Δ depends on the properties of relativistic turbulence. In any case, Δ if it determined by turbulence does not depend on microscopic plasma resistivity

and therefore the reconnection should be fast³ even if the scaling of turbulence in relativistic case differs from non-relativistic one.

On the basis of the recent studies of relativistic turbulence one may argue that LV99 model may be even directly applicable to the relativistic case. Indeed, the existing studies of the scaling and anisotropies of MHD turbulence (Cho 2008 and Cho & Lazarian 2012) testify that the relation between the parallel and perpendicular scales of eddies as well as the spectrum of turbulence are the same for relativistic and non-relativistic turbulence. As Δ in LV99 theory is determined by those properties of turbulence one can argue that the LV99 expressions for the reconnection rates can be directly relevant to relativistic reconnection⁴. This can be used at least as an educated guess for the discussion that we present further.

Irrespectively of the exact correspondence of the properties of relativistic and non-relativistic MHD turbulence one can argue that in the presence of turbulence Δ should increase and therefore the rate of magnetic reconnection should grow. This provides a prediction of flares of reconnection, explaining bursty energy release that is observed in solar flares as well as in many high energy phenomena, as it discussed in LV99. Indeed, if magnetic fluxes in contact are initially laminar or very weakly turbulent, Δ and therefore the reconnection rate may be slow initially. However this situation is unstable in the sense that if the outflow of plasma from the reconnection region gets turbulent, this will increase the turbulence of the ambient magnetic field and increase Δ . With larger Δ the outflow has larger Reynolds number and thus will get more turbulent. This results in "reconnection instability" (see more in Lazarian & Vishniac 2010). Similarly, one can argue that another process predicted in LV99 and reported in the observations by Sych et al. (2010), i.e. the initiation of reconnection by magnetic reconnection in adjacent regions should also be present in the relativistic case.

3.3.2. Acceleration at relativistic reconnection

Studies of the First order Fermi acceleration has been performed so far for non-relativistic reconnection (see de Gouveia dal Pino & Lazarian 2005, Lazarian 2005, Drake et al. 2006, Lazarian & Opher 2009, Drake et al. 2010, Lazarian & Desiati 2010, Lazarian et al. 2011, Kowal et al. 2012). We briefly summarize those below. The first order acceleration of particles entrained on the contracting magnetic loop can be understood from the Liouville theorem. In the process of the magnetic tubes contraction a regular increase of the particle's energies is expected. The requirement for the process to proceed efficiently is to keep the accelerated particles within the contracting magnetic loop. This introduces limitations on the particle diffusivity perpendicular to the magnetic field direction. The subtlety of the point above is related to the fact that while in the first-order Fermi acceleration in shocks magnetic compression is important, the acceleration via the LV99 reconnection process is applicable even to incompressible fluids. Thus, unlike shocks, it is not the entire volume that shrinks for the acceleration, but only the volume of the magnetic flux tube. Thus high perpendicular diffusion of particles may decouple them from the magnetic field. Indeed, it is easy to see that while the particles within a magnetic flux rope depicted in Figure 6 bounce back and forth between the converging mirrors and get accelerated, if these particles leave the flux rope fast, they may start bouncing between the magnetic fields of different flux ropes which may sometimes decrease their energy. Thus it is

³Magnetic reconnection is universally defined as fast when it does not depend on resistivity.

⁴One may question the application of the field wandering concept to relativistic case. However, LV99 expression for Δ (and therefore also reconnection rates) was re-derived in ELV11 without appealing to this concept.

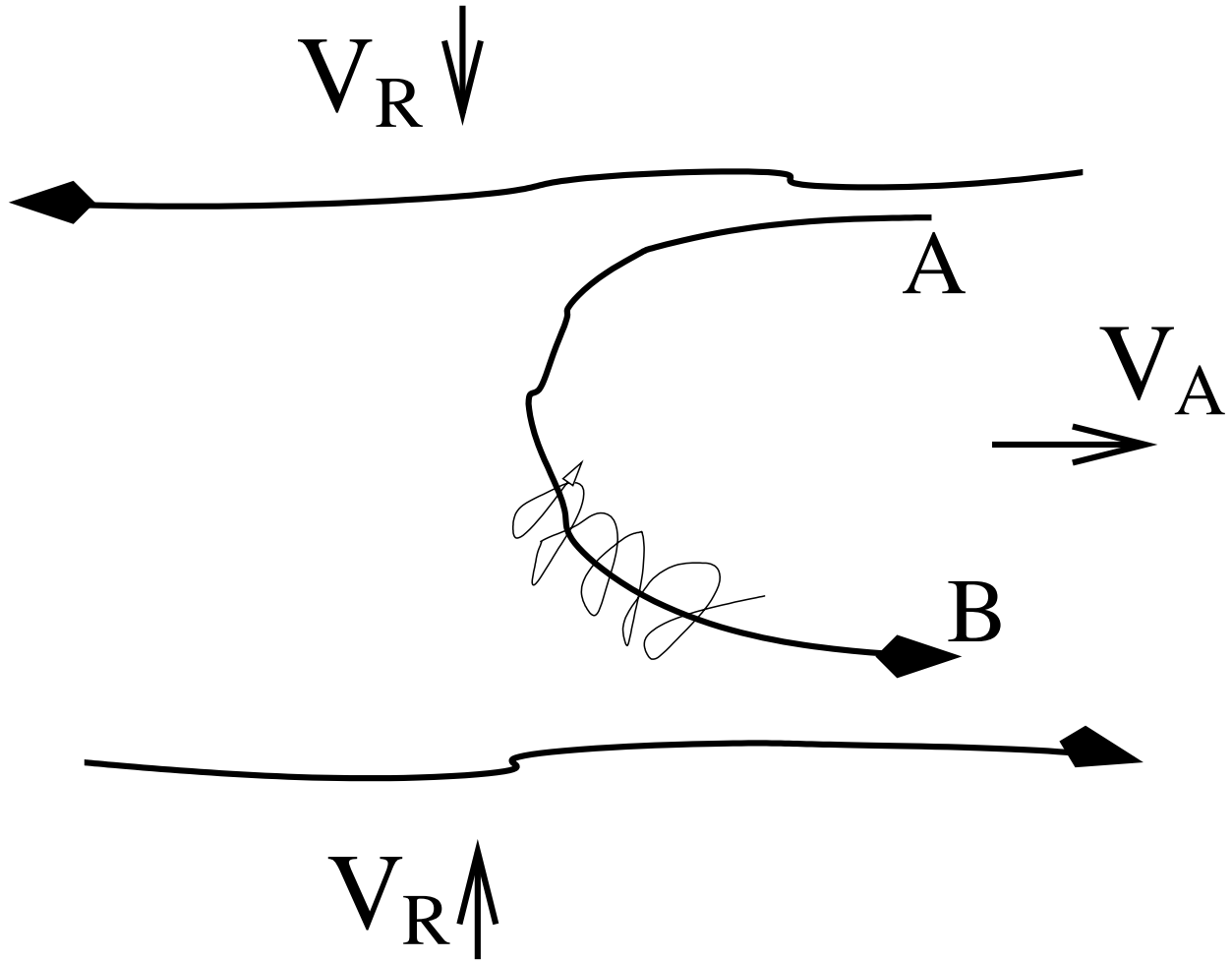


Fig. 6.— Cosmic rays spiral about a reconnected magnetic field line and bounce back at points A and B. The reconnected regions move towards each other with the reconnection velocity V_R . From Lazarian 2005.

important that the particle diffusion both in the parallel and perpendicular directions to the magnetic field stay different. The particle anisotropy which arises from particles preferentially getting acceleration in terms of the parallel momentum may also be important.

Similarly, the first order Fermi acceleration can happen in terms of the perpendicular momentum. This is illustrated in Figure 7. There the particle with a large Larmour radius is bouncing back and forth between converging mirrors of reconnecting magnetic field systematically getting an increase of the perpendicular component of its momentum. Both processes take place in reconnection layers.

3.4. Force-free turbulent cascade.

One of the most efficient ways of magnetic dissipation is through the turbulent cascade where the energy is transported from the large input scales to the small dissipation scales (Zakharov et al. 1992). The non-

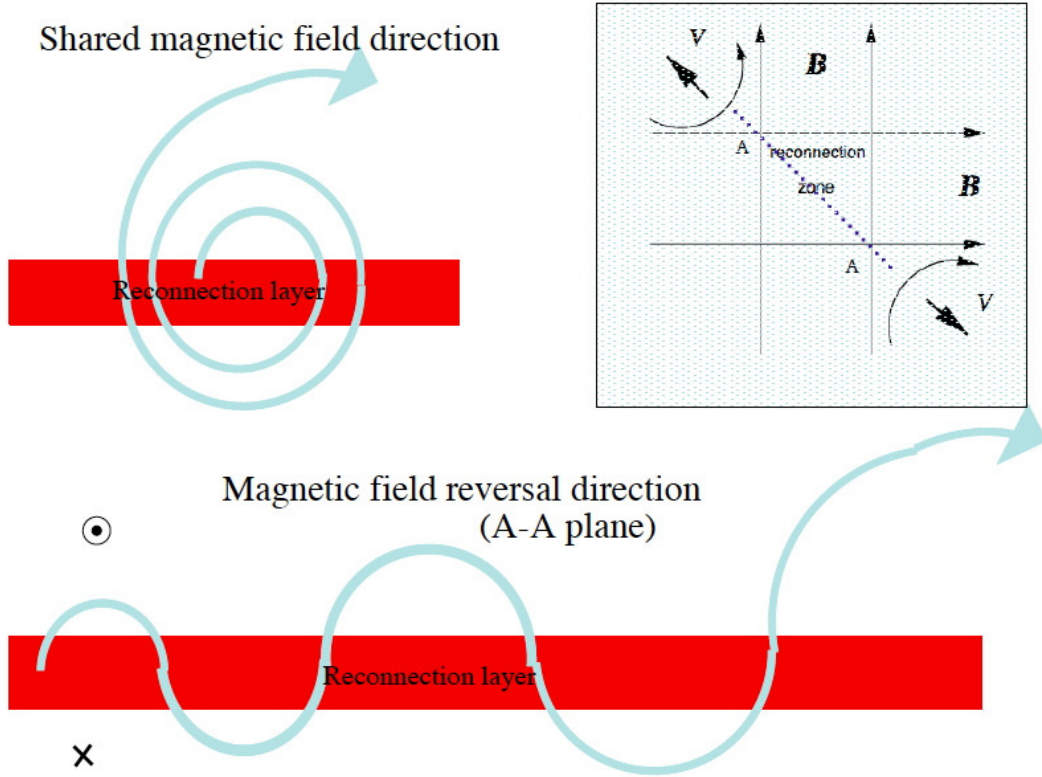


Fig. 7.— Particles with a large Larmor radius gyrate about the magnetic field shared by two reconnecting fluxes (the latter is frequently referred to as “guide field”. As the particle interacts with converging magnetized flow corresponding to the reconnecting components of magnetic field, the particle gets energy gain during every gyration. From Lazarian et al. 2012.

relativistic theory of turbulent cascade in magnetized plasma is in the stage of active development, both theoretical (Iroshnikov 1963; Kraichnan 1965; Montgomery & Turner 1981; Shebalin *et al.* 1983; Sridhar & Goldreich 1994; Goldreich & Sridhar 1997; Ng & Bhattacharjee 1996; Lazarian & Vishniac 1999; Galtier *et al.* 2000) and numerical (Maron & Goldreich 2001; Cho, Lazarian & Vishniac 2002; Cho & Lazarian 2002, 2003; Kowal & Lazarian 2010). The consensus that is emerging from these studies is that in the non-relativistic case the Alfvén wave cascade is well decoupled from the fast and slow modes due to the fact that Alfvén waves are incompressible (slow mode follows Alfvén waves). Unlike the hydrodynamic turbulence, the Alfvén wave cascade is anisotropic with energy cascading mostly perpendicularly to the magnetic field.

What is the structure of cascade in strongly magnetized plasma? First, we expect that like the traditional hydromagnetic turbulence the electromagnetic turbulence is local in phase space, so that the most important interaction is between waves with similar wave lengths. This is because the longer wavelength perturbations can be excluded via the relevant Lorentz transformation.

Previously, its properties have been addressed in Thompson & Blaes (1998); Troischt & Thompson (2004). Thompson & Blaes (1998) assumed that the relativistic Alfvén turbulence is similar to the non-

relativistic one thus the energy cascade remains anisotropic. However, this is unlikely to be true for the electromagnetic turbulence where the fast waves play an important role as the Alfvén waves. Indeed, there exists strong three-wave coupling between the non-zero frequency Alfvén waves and fast waves: $A + F \rightarrow A$, $A + F \rightarrow F$ and $A + A \rightarrow F$. In the non-relativistic case, the three wave coupling between non-zero frequency Alfvén waves and fast waves does not exist because the resonance condition cannot be satisfied, and the coupling between three fast waves does not exist because of the vanishing coupling coefficient.

The three wave interaction coefficients are complicated, with different dependences on the angles of interacting waves. Generically, the coupling of Alfvén and fast waves is strong, so that the two cascades are well coupled. Two important questions need to be answered: what are the angular dependence of the cascades and what are the wave number dependence. It is feasible that both cascades are anisotropic in such a way that the stationary kinetic equation for both Alfvén and fast waves are satisfied. We consider this unlikely. Alternative possibility, which we favor, is that the interaction of two cascades may isotropise them.

4. Step toward relativistic turbulence: vortical flows of relativistic fluid

Dynamics of relativistic plasma is a basic problem in fluid mechanics that has a wide range of applications from the physics of early Universe to heavy nuclei collisions to astrophysics. In cosmological applications, the post-inflation stage of reheating, that lead to matter creation, is dominated by relativistic turbulence (Micha & Tkachev 2003). In nuclear physics, the head-on collision of two highly relativistic nuclei creates a relativistically hot quarkgluon plasma that (Rischke et al. 1995). On a very different scale, a wide variety of astrophysical objects like jets from Active Galactic Nuclei (Begelman et al. 1984), Gamma Ray Bursts (Lyutikov 2006c) pulsar winds Kennel & Coroniti (1984) contain relativistic plasma.

Both, the quarkgluon plasma of nuclear collisions and astrophysical plasma are nearly ideal, with very small viscose contribution. Nearly ideal fluids are subject to the development of turbulence Landau & Lifshitz (1959). In the astrophysical set-up the relativistic turbulence may result in a dynamo action, that may be essential for the production of the high energy emission (Zhang et al. 2009). In addition, in case of relativistic supersonic flows the turbulence is necessarily for acceleration of cosmic rays at shocks Blandford & Eichler (1987).

Despite these important applications, the theory of relativistic turbulence is not developed, with only a few works addressing its statistical and dynamics properties (*e.g.* Dettmann & Frankel 1996; Goodman & MacFadyen 2008). Since the relativistic turbulence is generically compressive, we expect (following the analogy with the non-relativistic compressive turbulence) that the turbulence can be represented as a collection of interacting vortical and compressible modes. The compressible modes in the relativistic plasma are well known (*e.g.* Landau & Lifshitz 1959). On the other hand, the vortical modes in the relativistic fluid has not been considered so far.

One of the key features of relativistic vortices is that the flow compressibility must be taken into account. This makes a majority of work on vortices, which often use a non-compressible approximation, (Landau & Lifshitz 1959; Lamb 1975), not applicable to relativistic vortices. On the other hand, relativistic vortices resemble in many ways the vortices in the compressible fluids Green (1995). The centrifugal forces “pull away” gas from the axis and can lead to the development of a cavitated core. First we consider a structure of simple rectilinear relativistic vortex. A simple rectilinear vortex with zero distributed vorticity has the

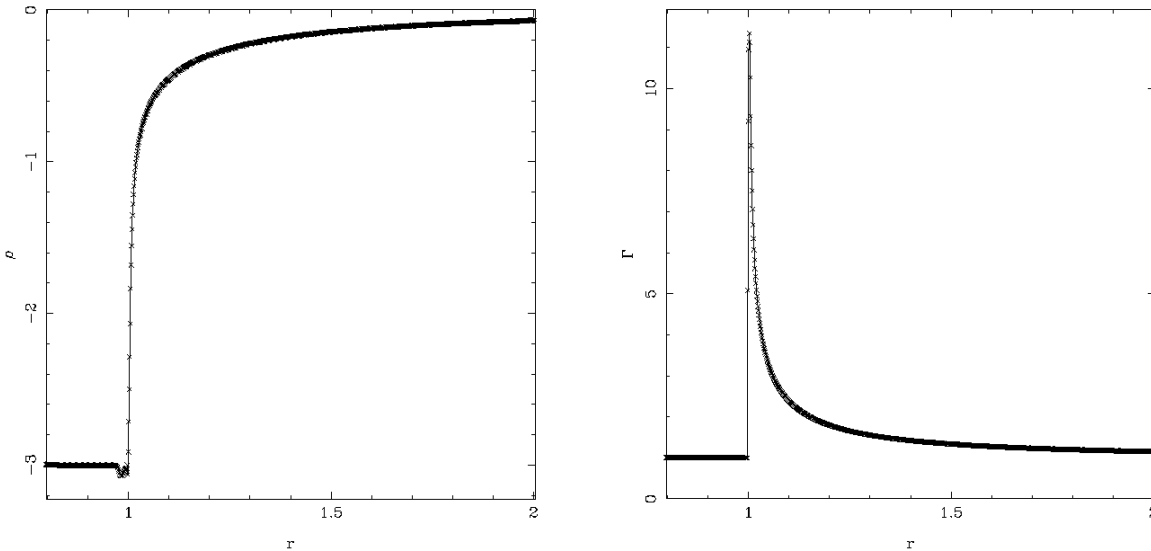


Fig. 8.— Structure of relativistic vortex: proper density and Lorentz factor. One clearly sees a cavitated core. The inside of the vortex had to be filled with dynamically unimportant low density gas since the scheme does not allow full cavitation.

following four-velocity structure:

$$u_\phi = \frac{1}{\sqrt{(r/r_0)^2 - 1}} \quad (13)$$

For polytropic equation of state with index Γ the density becomes zero at

$$r_i = \frac{1 + \Gamma\kappa_\infty}{\sqrt{\Gamma\kappa_\infty(2 + \Gamma\kappa_\infty)}} \frac{\Gamma_z}{2\pi\tilde{w}_\infty} \quad (14)$$

where κ_∞ and \tilde{w}_∞ are vorticity and proper enthalpy measured at infinity. Thus, a simple relativistic vortex is cavitated - it has an empty vacuum core.

Vortical flows must have cores with special properties that are different from the bulk flow. The structure of the core of the both relativistic and non-relativistic vortices depends both on the parameters of the system and the history how a vortex has been created. Formally, for realistic isentropic EoS the rectilinear relativistic vortex develops a cavitated core. The development of the cavitated core occurs in the non-relativistic compressible fluid as well. For a typical laboratory fluid vortex with highly subsonic flow $M \ll 1$ and not exceptionally high Reynolds numbers Re , the viscous core forms on time of the order of the dynamical time. On the other hand, in astrophysics we expect $M \sim 1$, while the Reynolds number Re is huge. Thus, in astrophysical conditions the formation time of a viscous core is very long, so that, generically, an isolated rectilinear astrophysical vortex will be cavitated.

5. The subtle role of global electric fields

Astrophysical plasmas, typically, do not tolerate large scale electric fields: charge non-neutrality in highly conducting medium is quickly suppressed by drawing-in of the opposite charges. As a result, the dynamical role of large-scale electric fields in the overall dynamics and particle acceleration is often underappreciated. Magnetic fields, on the other hand, may both suppress charge neutralization and can themselves give rise to global inductive electric fields. Below we discuss two cases where global inductive electric fields and charge non-neutral plasma may be important in otherwise conventional plasmas.

5.1. Inductive Acceleration of UHERCs

Relativistic outflows carrying large scale magnetic fields have large inductive potential and may accelerate protons to ultra high energies. Lyutikov & Ouyed (2007) discussed a scheme of Ultra-High Energy Cosmic Ray (UHECR) acceleration due to drifts in magnetized, cylindrically collimated, sheared jets of powerful active galaxies.

Lyutikov & Ouyed (2007) model of UHECR acceleration relies on the observation that in a transversely sheared flow one sign of charges is located at a maximum of electric potential, as we describe in this section. Consider sheared flow carrying magnetic field. At each point there is electric field $\mathbf{E} = -\mathbf{v} \times \mathbf{B}/c$, so that the electric potential is determined by

$$\Delta\Phi = \frac{1}{c}\nabla \cdot (\mathbf{v} \times \mathbf{B}) = \frac{1}{c}(\mathbf{B} \cdot (\nabla \times \mathbf{v}) - \mathbf{v} \cdot (\nabla \times \mathbf{B})) \quad (15)$$

If system is stationary and current-free, (in a local rest frame, the second term in Eq. (15) vanishes at the position of a particle and is generally sub-dominant to the first term in the near vicinity) then $\nabla \times \mathbf{B} = 0$ and we find

$$\Delta\Phi = \frac{1}{c}(\mathbf{B} \cdot \nabla \times \mathbf{v}) \quad (16)$$

We have arrived at an important result: *depending on the sign of the quantity $(\mathbf{B} \cdot \nabla \times \mathbf{v})$ (which is a scalar) charges of one sign are near potential minimum, while those with the opposite sign are near potential maximum.* Since electric field is perpendicular both to velocity and magnetic field, locally, the electric potential is a function of only one coordinate along this direction. For $(\mathbf{B} \cdot \nabla \times \mathbf{v}) < 0$ ions are near potential maximum. A positively charged particle carried by such a plasma is in an unstable equilibrium if $\mathbf{B} \cdot \nabla \times \mathbf{v} < 0$, so that kinetic drift along the velocity shear would lead to fast, *regular* energy gain.

The procedure outlined above to calculate electric potential is beyond the limits of applicability of *non-relativistic* MHD, which assumes quasi-neutrality and thus neglects the dynamical effects associated with the potential (16). Thus, even in the low frequency regime with non-relativistic velocities, a conventional realm of MHD theory, one should use at least two fluid approach and also must retain both charge density as well as displacement current in Maxwell equations.

Under ideal fluid approximation particles cannot move across magnetic fieldlines, so that they cannot “sample” the electric potential (16). On the other hand, kinetic effects, like drift motions, may lead to regular radial displacement along the shear and thus along electric field. In this case one sign of charge will be gaining energy, while another sign will be losing energy. This is independent on whether the drift is along the shear or counter to the shear direction and thus is independent on the sign of the magnetic fieldgradient that induces the shear.

When the Larmor radius becomes comparable to shear scale the particle motion becomes unstable even for homogeneous flow. Particle trajectories can be found in quadratures in the general case Lyutikov & Ouyed (2007). In the non-relativistic limit equations of motion can be integrated exactly,

$$y = r_L \cos Z\omega_B \sqrt{1 + \eta/Z\omega_B t}, z = -\frac{r_L}{\sqrt{1 + \eta/Z\omega_B}} \sin Z\omega_B \sqrt{1 + \eta/Z\omega_B t} \quad (17)$$

where $\eta = V'$. This clearly shows that for strong negative shear, $\eta < -\omega_B$, particle trajectory is unstable and its energy growth exponentially. For positive shear, $\eta > 0$, particle motion is stable.

5.2. Relativistic effects at cosmic ray-modified perpendicular shocks

Acceleration of cosmic rays is one of the main problems of high energy astrophysics. Shock acceleration is the leading model (Blandford & Eichler 1987). Particle acceleration at quasi-parallel shocks (when the magnetic field in the upstream medium is nearly aligned with the shock normal) and quasi-perpendicular shocks (when the magnetic field in the upstream medium is nearly orthogonal to the shock normal) proceeds substantially differently. Most astrophysical shocks are quasi-perpendicular, yet theoretically acceleration at this type of shocks is less understood than in the case of quasi-parallel shocks. It is recognized that the feedback of accelerated cosmic rays may considerably modify the parallel shock structure (Axford et al. 1982).

Kinetic diffusion of cosmic rays ahead of perpendicular shocks induces large scale charge non-neutrality, which is typically neglected in the non-relativistic fluid approach. Cosmic rays diffusing ahead of the shock offset the charge balance in the incoming plasma, which becomes non-neutral, with electric field directed along the shock normal. The incoming upstream plasma will *partially* compensate this charge density by a combination of electric and polarization drifts. This creates a current along the shock normal, perpendicular to the magnetic field, see Fig. 9. Current-driven instabilities, in particular of the modified Buneman type, generate plasma turbulence with wave vectors preferentially perpendicular to the initial magnetic field, generating the field line wandering required for acceleration of cosmic rays in the first place. Thus, similar to parallel shocks, assumption of turbulence and cosmic ray acceleration leads to turbulence generation by cosmic rays themselves Lyutikov (2010b).

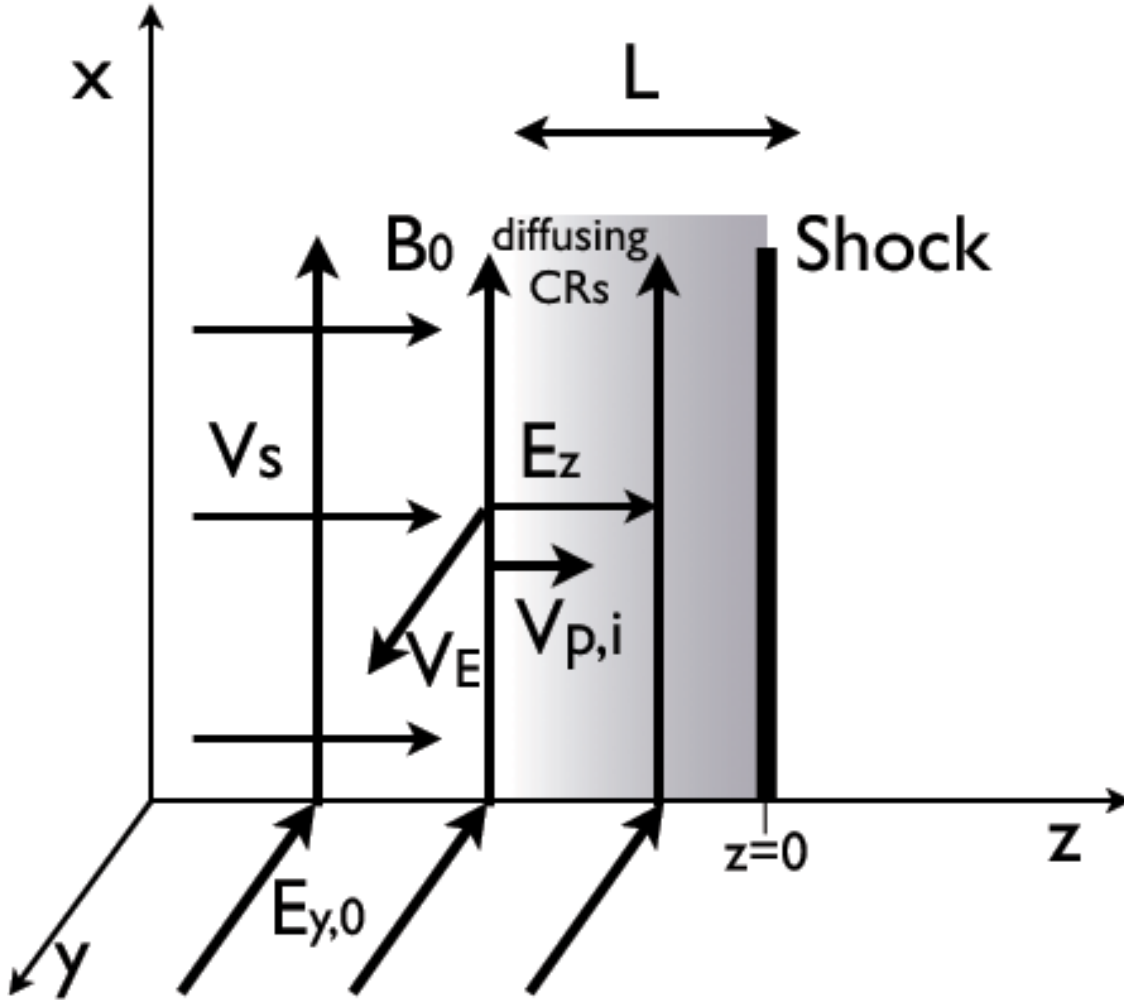


Fig. 9.— Plasma flows in the frame of the shock. Far upstream, the incoming plasma moves with velocity v_s , magnetic field is along x direction and inductive electric field along $-y$ direction. At the shock, cosmic rays are accelerated and diffuse ahead of the shock a typical distance L , creating an electric field along the shock normal. Electric drift of cosmic rays in this induced electric field and the initial magnetic field produces z -dependent electric drift v_E in y direction. Acceleration of plasma in y direction in turn produces polarization drift of ions in z direction.

REFERENCES

- Abdo et al. 2011, *Science*, 331, 739
 Aharonian, F. *et al.*. 2007, *ApJ*, 664, L71
 Albert, J. *et al.*. 2007, *ApJ*, 669, 862
 Antiochos, S. K. and DeVore, C. R. and Klimchuk, J. A. , 1999, *ApJ*, 510, 485

- Aschwanden, M. J., 2002, *Space Science Reviews*, 101, 1
- Aschwanden, M. J. 2005, *Physics of the Solar Corona. An Introduction with Problems and Solutions* (2nd edition)
- Axford, W. I., Leer, E., & McKenzie, J. F. 1982, *A&A*, 111, 317
- Begelman, M. C., Blandford, R. D., & Rees, M. J. 1984, *Reviews of Modern Physics*, 56, 255
- Begelman M. C., 1998, *ApJ*, 493, 291
- Uzdensky, D., Cerutti, B., & Begelman, M. 2011, *The Astrophysical Journal Letters*, 737
- Blandford, R. & Eichler, D. 1987, *Phys. Rep.*, 154, 1
- Birdsall, C.K., Langdon, A.B., 1991, 'Plasma Physics via Computer Simulation', IOP, Bristol, United Kingdom
- Biskamp, D. 2000, "Magnetic Reconnection in Plasmas", Cambridge University Press, Cambridge
- Field, G. B. 1994, *Physical Review Letters*, 72, 494,
- Blandford, R.D., & Znajek, R.L. 1977, *MNRAS*, 179, 433
- Blandford, R.D. & Payne, D.G. 1982, *MNRAS*, 199, 883
- Błażejowski, M., *et al.* , 2005, *ApJ*, 630, 130
- Buehler et al. 2012, *ApJ*, 749, 26
- Cho, J., & Lazarian, A. 2002, *Physical Review Letters*, 88, 245001
- Cho, J., & Lazarian, A. 2003, *MNRAS*, 345, 325
- Cho, J. and Lazarian, A. and Vishniac, E. T., 2002, *ApJ*, 564, 291
- Clausen-Brown, E. & Lyutikov, M. 2012, *MNRAS*, 426, 1374
- Coburn, W., & Boggs, S.E. 2003, *Nature*, 423, 415
- Coroniti, F. V. 1990, *ApJ*, 349, 538
- Cowley, S. C. and Artun, M., 1997, *Phys. Rep.*, 283, 185
- Dedner, A. *et al.* , (2002), *Journal of Computational Physics*, 175, 645
- Dettmann, C. P. & Frankel, N. E. 1996, *Phys. Rev. E*, 53, 5502
- De Villiers, J.-P. and Hawley, J. F. and Krolik, J. H. and Hirose, S., 2005, *ApJ*, 620, 878
- de Jager, O. C., , A. K., Michelson, P. F., Nel, H. I., Nolan, P. L., Sreekumar, P., & Thompson, D. J. 1996, *ApJ*, 457, 253
- de Gouveia dal Pino, E. M., & Lazarian, A. 2005, *A&A*, 441, 845
- Drake, J. F., Swisdak, M., Che, H., & Shay, M. A. 2006, *Nature*, 443, 553

- Dungey, J. W. 1953, MNRAS, 113, 180
- Espinoza C. M., Jordan C., Stappers B. W., Lyne A. G., Weltevrede P., Cognard I., Theureau G., 2010, The Astronomer’s Telegram, 2889, 1
- Eyink, G. L., Lazarian, A., & Vishniac, E. T. 2011, ApJ, 743, 51 (ELV11)
- Ferrari, A., 2004, Ap&SS, 293, 15
- Galeev, A. A., Coroniti, F. V., Ashour-Abdalla, M. , 1978, Geophys. Res. Lett., 5, 707
- Gabuzda, D.C., & Murray, É. 2003, Proceedings of the Conference “Future Directions in High Resolution Astronomy: A Celebration of the 10th Anniversary of the VLBA”, Socorro, USA
- Galtier, S., Nazarenko, S. V., Newell, A. C., Pouquet, A. 2000, J. Plasma Phys., 63, 447
- Gruzinov, A. 1999, ArXiv Astrophysics e-prints
- . 2007, ArXiv e-prints
- . 2012, ArXiv e-prints
- Ghisellini, G. & Tavecchio, F. 2008, MNRAS, 386, L28
- Giannios, D., Uzdensky, D. A., & Begelman, M. C. 2009a, MNRAS, 395, L29
- . 2009b, MNRAS, 395, L29
- . 2010, MNRAS, 30
- Goodman, J. & MacFadyen, A. 2008, Journal of Fluid Mechanics, 604, 325
- Green, S. I. 1995, Fluid Vortices (Springer)
- Göğüş , E., Woods, P. M., Kouveliotou, C., van Paradijs, J., Briggs, M. S., Duncan, R. C., & Thompson, C. 1999, ApJL, 526, L93
- Goldreich, P. and Sridhar, S., 1997, ApJ, 485, 680
- Hoshino, M. & Lyubarsky, Y. 2012, Space Sci. Rev., 78
- Iroshnikov, P. 1963, Soviet Astron., 7, 566
- Kadomtsev, B. B., 1975, Soviet Journal of Plasma Physics, 1, 710
- Kennel, C. F. & Coroniti, F. V. 1984, ApJ, 283, 694
- Kumar, P. & Narayan, R. 2009, MNRAS, 395, 472
- Komissarov S.S., 1999, MNRAS, 303, 343.
- Komissarov S.S., 2002, MNRAS, 336, 759.
- Komissarov S.S., 1999, MNRAS, 308, 1069.
- Komissarov S.S., 2001, MNRAS, 326, L41.

- Komissarov S.S., 2004, MNRAS, 350, 427.
- Komissarov S.S., 2006, MNRAS, 367, 19.
- Komissarov, S. S., Barkov, M., & Lyutikov, M. 2007, MNRAS, 374, 415
- Komissarov S.S., Lyubarsky Y.E., 2003, MNRAS, 344, L93.
- Komissarov S.S., Barkov M., Vlahakis N., Konigle A., 2007b, MNRAS submitted (astro-ph/0703146)
- Komissarov S.S., McKinney J.C., 2007, MNRAS, 377, L49
- Komissarov, S. S. 2012, ArXiv e-prints, 1207.3192
- Kowal, G., & Lazarian, A. 2010, ApJ, 720, 742
- Kraichnan, R. 1965, Phys. Fluids, 8, 1385
- Lovelace, R. V. E., Li, H., Koldoba, A. V., Ustyugova, G. V., & Romanova, M. M. 2002, ApJ, 572, 445
- . 2005, MNRAS, 358, 113
- Lamb, H. 1975, Hydrodynamics (Cambridge: Cambridge University Press, 1975, 6th ed.)
- Landau, L. D. & Lifshitz, E. M. 1959, Fluid mechanics (Oxford: Pergamon Press, 1959)
- Lazar, A., Nakar, E., & Piran, T. 2009, ApJ, 695, L10
- Lazarian, A. 2005, Magnetic Fields in the Universe: From Laboratory and Stars to Primordial Structures., 784, 42
- Lazarian, A. 2006, ApJL, 645, L25
- Lazarian, A., Kowal, G., Vishniac, E., & de Gouveia Dal Pino, E. 2011, Planetary and Space Science, 59, 537
- Lazarian, A., & Desiati, P. 2010, ApJ, 722, 188
- Lazarian, A., & Opher, M. 2009, ApJ, 703, 8
- Lazarian, A., Petrosian, V., Yan, H., & Cho, J. 2003, arXiv:astro-ph/0301181
- Lazarian, A., & Vishniac, E. T. 1999, ApJ, 517, 700
- Lazarian, A., Vishniac, E. & Cho, J. 2004, ApJ, 603, 180
- Lazarian, A., Vlahos, L., Kowal, G., Yan, H., Beresnyak, A., de Gouveia Dal Pino E. 2012, Space Science Review, DOI 10.1007/S 11214-9934-7
- Lazarian, A., & Yan, H. 2012, American Institute of Physics Conference Series, 1505, 101
- Lehner, L., Palenzuela, C., Liebling, S. L., Thompson, C., & Hanna, C. 2011, ArXiv e-prints
- Lister, M. L. *et al.*. 2009, AJ, 138, 1874
- Loureiro, N. F., Schekochihin, A. A., & Cowley, S. C. 2007, Physics of Plasmas, 14, 100703

- Lyubarsky, Y. E. 2003, MNRAS, 345, 153
- Lyutikov, M. 2006a, MNRAS, 369, L5
- Lyutikov, M. & Ouyed, R. 2007, Astroparticle Physics, 27, 473
- . 2010, MNRAS, 405, 1809
- . 2010b, MNRAS, 407, 1721
- . 2006b, MNRAS, 369, L5
- . 2006c, New Journal of Physics, 8, 119
- Lyutikov, M. & Uzdensky, D. 2003, ApJ, 589, 893
- Lyutikov, M., 2002, ApJ, 580, 65
- Lyutikov, M., 2003, MNRAS, 346, 540
- Lyutikov, M., Uzdensky D., 2003, ApJ, 589, 893
- Lyutikov M., Blandford R., 2003, astro-ph/0312347
- Lyutikov, M., Pariev, V., Blandford, R., 2003, ApJ, 597, 998
- Lyutikov, M., Gavriil, F., 2005, MNRAS, 368, 690
- Lyutikov, M., Pariev, V.I., & Gabuzda, D. 2003, “Polarization in Parsec Scale Radio Jets with Toroidal Magnetic Fields”, 2005, MNRAS, 360, 869
- Lyutikov, M., Thompson, C., 2005, ApJ, 634, 1223
- Lyutikov, M., 2006, MNRAS, 367, 1594
- Lyutikov M., 2006, New Journal of Physics, 8, 119
- . 2011, Phys. Rev. D, 83, 124035
- Lyutikov, M. & McKinney, J. C. 2011, Phys. Rev. D, 84, 084019
- Maron, J. and Goldreich, P., 2001, ApJ, 554, 1175
- Matthaeus, W. H., & Lamkin, S. L. 1985, Physics of Fluids, 28, 303
- Matthaeus, W. H., & Lamkin, S. L. 1986, Physics of Fluids, 29, 2513
- McKinney, J. C. and Gammie, C. F., 2004, ApJ, 611, 977-995
- McKinney, J. C. & Uzdensky, D. A. 2012, MNRAS, 419, 573
- Micha, R. & Tkachev, I. I. 2003, Physical Review Letters, 90, 121301
- McLaughlin, M. A., 2004, ApJ, 613, 57
- McLaughlin, M. A., et al. 2004, ApJ, 616, 131

- Mereghetti, S. *et al.*, 2005, ApJ, 628, 938
- Michel F.C. 1971, Comments Ap. Space Phys. 3, 80
- Montgomery, D., & Turner, L. 1981, Phys. Fluids, 24, 825
- Ng, C. S. and Bhattacharjee, A., 1996, ApJ, 465, 845
- Palmer, D. M. *et al.*, 2005, Nature, 434, 1107
- Piner, B. G., 2005, ASP Conf. Ser. 340: Future Directions in High Resolution Astronomy, 55
- Priest, E., & Forbes, T. 2000, “Magnetic Reconnection: MHD Theory and Applications”, Cambridge University Press, New York
- Priest, E. R. and Forbes, T. G., 2002, A&A Rev., 10, 313
- Rea, N. and Tiengo, A. and Mereghetti, S. and Israel, G. L. and Zane, S. and Turolla, R. and Stella, L., 2005, ApJ, 627, 133
- Rees, M. J., Gunn, J. E., 1974, MNRAS, 167, 1
- Rees, M. J. 1966, Nat, 211, 468
- Rischke, D. H., Bernard, S., & Maruhn, J. A. 1995, Nuclear Physics A, 595, 346
- Rutledge, R., Fox, D., 2003, MNRAS, 350, 1288
- Sauty, C., Tsinganos, K., & Trussoni, E. 2002, Lecture Notes in Physics, 589, 41
- Sikora, M. and Begelman, M. C. and Madejski, G. M. and Lasota, J.-P., 2005, ApJ, 625, 72
- Shebalin, J. V., Matthaeus, W. H., Montgomery, D. 1983, J. Plasma Phys., 29, 525
- Shivamoggi, B. K., 1985, Ap&SS,114,15
- Sridhar, S. and Goldreich, P., 1994, ApJ, 432, 612
- Spruit, H.C., Daigne, F., Drenkhahn, G., 2001, A&A, 369, p.694 –705
- Imshennik, V. S. & Syrovatskivi, S. I. 1967, Soviet Journal of Experimental and Theoretical Physics, 25, 656
- Li, J., Spitkovsky, A., & Tchekhovskoy, A. 2012, ApJ, 746, 60
- Tavani et al. 2011, Science, 331, 736
- Tchekhovskoy, A. & Spitkovsky, A. 2012, ArXiv e-prints
- Tiengo, A. and Esposito, P. and Mereghetti, S. and Rea, N. and Stella, L. and Israel, G. L. and Turolla, R. and Zane, S. , 2005, astro-ph/0508074
- Thompson, C. & Blaes, O. 1998, Phys. Rev. D, 57, 3219
- Thompson, C. & Duncan, R.C. 1995, MNRAS, 275, 255 (TD95)
- Thompson, C. & Duncan, R.C. 2001, ApJ, 561, 980 (TD01)

- Thompson, C., Lyutikov, M., Kulkarni, S. R., 2002, *ApJ*, 574, 332
- Tsyganenko, N., 2005, <http://modelweb.gsfc.nasa.gov/magnetos/data-based/modeling.html>
- Troischt, P. and Thompson, C., 2004, *Phys. Rev. D*, 70, 124030
- Willis, D. R. and Barlow, E. J. and Bird, A. J. and Clark, D. J. and Dean, A. J. and McConnell, M. L. and Moran, L. and Shaw, S. E. and Sguera, V., 2005, *A&A*, 439, 245
- Woods, P. M. and Kouveliotou, C. and Göğüş, E. and Finger, M. H. and Swank, J. and Smith, D. A. and Hurley, K. and Thompson, C., 2001, *ApJ*, 552, 748
- Woods, P. M. and Thompson, C., 2004, *astro-ph/0406133*
- Uzdensky, D. A., Cerutti, B., & Begelman, M. C. 2011, *ApJ*, 737, L40+
- Uzdensky, D. A. 2003, *ApJ*, 598, 446
- Zakharov, V. E., L'Vov, V. S., & Falkovich, G. 1992, *Kolmogorov spectra of turbulence I: Wave turbulence* (Springer Series in Nonlinear Dynamics, Berlin: Springer, 1992)
- Zhang, W., MacFadyen, A., & Wang, P. 2
- Zhang, B., & Yan, H. 2011, *ApJ*, 726, 90